Aromatic Pathways in Twisted Hexaphyrins

ARTICLE *in* THE JOURNAL OF PHYSICAL CHEMISTRY A · JULY 2010

Impact Factor: 2.69 · DOI: 10.1021/jp1021517 · Source: PubMed

4 AUTHORS:

Heike Fliegl
University of Oslo
36 PUBLICATIONS **846** CITATIONS
SEE PROFILE

Dage Sundholm
University of Helsinki
205 PUBLICATIONS **4,615** CITATIONS
SEE PROFILE

Stefan Taubert
University of Helsinki
17 PUBLICATIONS **333** CITATIONS
SEE PROFILE

Fabio Pichierri
Tohoku University
110 PUBLICATIONS **886** CITATIONS
SEE PROFILE

Aromatic Pathways in Twisted Hexaphyrins

Heike Fliegl,*,†,§ Dage Sundholm,*,† Stefan Taubert,*,† and Fabio Pichierri*,‡

Department of Chemistry, P.O. Box 55 (A.I. Virtanens plats 1), FIN-00014 University of Helsinki, Finland, G-COE Laboratory, Department of Applied Chemistry, Graduate School of Engineering, Tohoku University, Aoba-yama 6-6-07, Sendai, 980-8579 Japan, and Karlsruhe Institute of Technology, Institute of Nanotechnology Hermann-von-Helmholtz-Platz 1, D-76344 Eggenstein-Leopoldshafen, Germany

Received: March 10, 2010; Revised Manuscript Received: May 13, 2010

The aromatic pathways and the degree of aromaticity of expanded porphyrins have been determined by explicit calculations of the routes and strengths of the magnetically induced currents using the gauge-including magnetically induced current (GIMIC) approach. Density functional theory calculations show that the doubly twisted hexaphyrins fulfilling Hückel's $(4n + 2)$ π-electron rule for aromaticity and those obeying the $4n$ π-electron rule for antiaromaticity are aromatic and antiaromatic, respectively. The investigated [26]hexaphyrin (**2**) and (**3**) and [30]hexaphyrin (**5**) isomers are aromatic, and [28]hexaphyrin (**4**) is antiaromatic. The formally antiaromatic [24]hexaphyrin (**1**) does not sustain any strong ring current and must be considered nonaromatic. A detailed analysis of the current pathways of the hexaphyrins is presented. It was found that the current pathways of the investigated aromatic hexaphyrins are not always dominated by the flow along the inner route through the non-hydrogenated C—N—C moieties, as previously proposed. The current flow is often split into two branches at the pyrrole rings, but sometimes it takes the outer route via the C═C bond of the pyrrole. The current pathway of the weak paratropic ring current of [24]hexaphyrin is dominated by the outer C═C route. The calculations show that the routes of the current transport cannot be assessed merely by inspection or from nucleus independent chemical shifts; explicit calculations of the current pathways are compulsory. The current-density studies also show that the pyrrole rings do not sustain any strong ring currents of their own.

1. Introduction

In aromatic planar molecules an external magnetic field perpendicular to the molecular plane induces a diatropic ring current, generating a magnetic field opposing the applied field. In antiaromatic molecules the induced current circulates in the opposite, paratropic direction, thus strengthening the external magnetic field. Calculation of the strength of the magnetically induced ring current is an accurate method to determine the degree of aromaticity according to the magnetic criterion.[1−4] The development of new computational tools such as the gauge-including magnetically induced current (GIMIC) method renders unambiguous calculations of current pathways and current strengths feasible.[1] The current pathway, the current strength, and the direction of the magnetically induced currents obtained in the current calculations can be used to characterize the aromatic properties of complex multiring molecules.[1,5−7]

Here, we investigate the molecular aromaticity and the current pathways of meso-trifluoromethyl-substituted hexaphyrin rings. The calculated strengths of the magnetically induced currents passing through selected bonds are used to assess the degree of aromaticity of the [24]hexaphyrin, [26]hexaphyrin, [28]hexaphyrin, and [30]hexaphyrin molecules, shown in Figure 1. These porphyrinoid molecules differ from each other by having different numbers of hydrogen atoms bonded to the pyrrole nitrogens. The current densities are obtained using the GIMIC method,[1] which has previously been applied in studies of current strengths and pathways of molecular systems.[5−10] Numerical integration of the current density passing specific bonds yields unambiguous electron-delocalization pathways characterizing the molecular aromaticity properties of the investigated hexaphyrins. The ring-current strengths around the hexaphyrins are used to determine the degree of aromaticity.

The Möbius class of molecules can be generalized to comprise multiply twisted molecular rings, the topology of which can be analyzed using modern mathematical methods.[11−15] Conventional Möbius molecules having a two-dimensional (2D) center line are characterized by a 180° twist around the ring.[16] Classical Hückel molecules are known for being largely planar with a topology linking number of zero. Generally, Möbius molecules are twisted by $n\pi$ radians around the ring, where n is a nonzero integer.[16] The Möbius twist of the molecular ring significantly affects the electronic structure. For example, conjugated molecules with Hückel and conventional 2D Möbius topology have different π-electron count rules for aromaticity. Hückel's rule for aromaticity states that conjugated rings with $(4n + 2)$ π -electrons are aromatic.[17,18] Molecules with conventional 2D Möbius topology have the π orbitals twisted by π radians along the conjugation pathway of the molecular ring.[19−22] They are single-sided and have been suggested to be aromatic when the number of π-electrons is $4n$.[23−26]

The Möbius aromaticity rules can be extended to multiply twisted molecular rings having a nonplanar 3D center line. Molecules with a linking number (L_k) proportional to an even integer times π are aromatic, when fulfilling the $(4n + 2)$ π-electron condition. Molecules with a twisted ring corresponding to an odd L_k value times π are aromatic when having $4n$

* To whom correspondence should be addressed. E-mail: Heike.Fliegl@helsinki.fi (H.F.); Dage.Sundholm@helsinki.fi (D.S.); Stefan.Taubert@helsinki.fi (S.T.); fabio@che.tohoku.ac.jp (F.P.).
† University of Helsinki.
‡ Tohoku University.
§ Karlsruhe Institute of Technology.

10.1021/jp1021517
Published on Web 06/16/2010

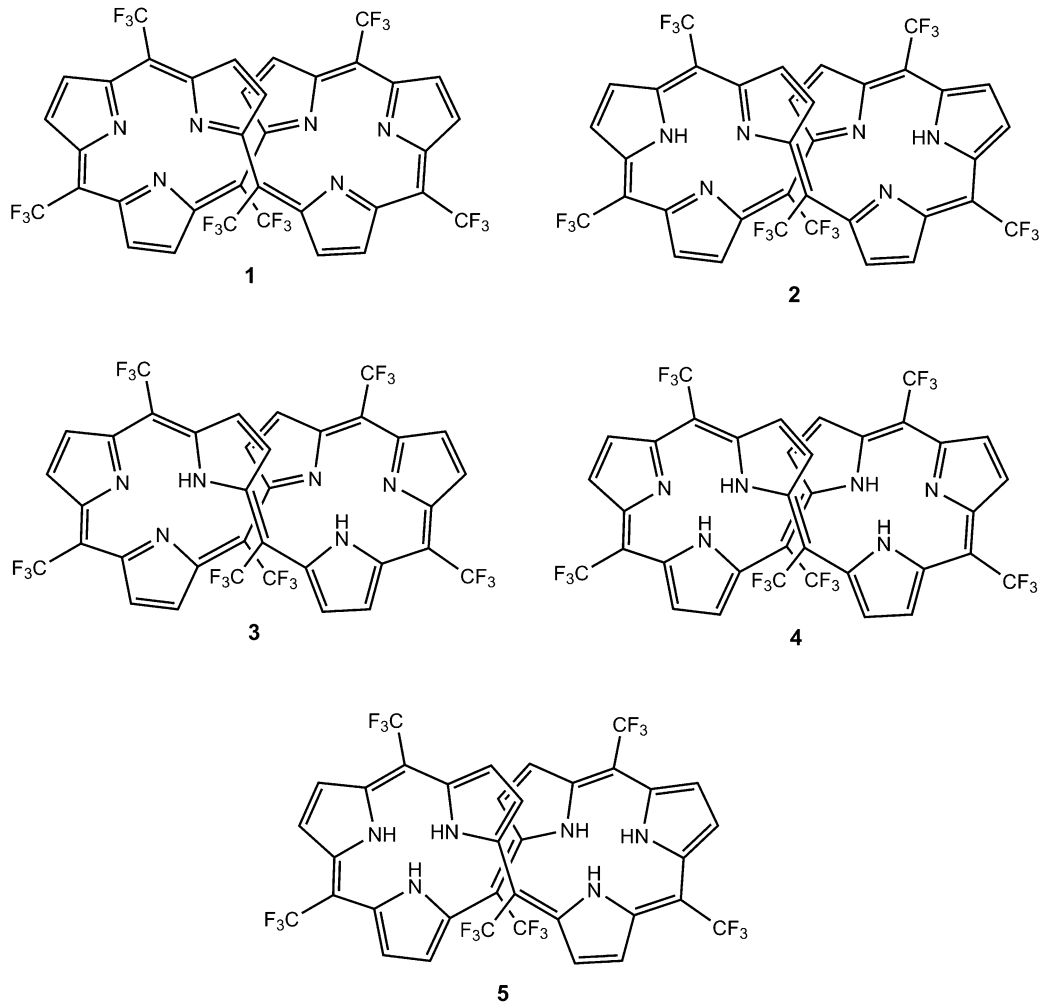

Figure 1. The molecular structures of the investigated hexaphyrin isomers represented as 2D projections.

π-electrons.[16] Antiaromaticity can analogously be expected for molecular rings with $4n$ π-electrons and even L_k or when the number of π-electrons is $(4n + 2)$ and L_k is odd. The linking number consists of the twisting number (T_w), which is a local property, and the nonlocal writhing number (W_r). The linking, twisting, and writhing numbers are related through $L_k = T_w + W_r$.[12−15] For molecular rings, T_w is a sum of the local relative twists of the atoms in the molecular ring. Thus, T_w correlates with the overlap of the atomic p orbitals of neighboring atoms, whereas W_r is related to the strain of the molecular ring. The larger the W_r the sharper is the curvature of the molecular loop corresponding to a larger ring strain.

Many attempts to synthesize Möbius annulenes have been reported throughout the years. In 2003, Herges et al. claimed that they had synthesized the first aromatic Möbius annulene with 16 π-electrons.[19,20,22] However, nucleus independent chemical shifts (NICS) calculations by Castro et al. indicated that it is nonaromatic.[27] Our recent calculations of the strength of the magnetically induced ring current showed indeed that both the Möbius and the Hückel structures of the bianthraquinodimethane-stabilized [16]annulene must be considered nonaromatic as the [16]annulene rings have very small ring-current susceptibilities of 0.3 nA/T or about 2.5% of the benzene value.[9,10]

The severe difficulties encountered in the synthesis of Möbius-stabilized annulenes could be circumvented when realizing the possibility of generating Möbius strips and multiply twisted molecular rings consisting of conjugated pyrrole units.[28−32] Therefore, expanded porphyrins have recently received great interest.[33] Stepień et al. found that the NMR chemical shifts of expanded porphyrins and porphyrinoids are strongly temperature dependent suggesting an equilibrium between structures with Möbius and Hückel topology.[34−36] The NMR measurements showed that the Möbius structure dominates at low temperatures and that the Hückel structure prevails at higher ones. Sankar et al. studied meta-substituted [28]hexaphyrins spectroscopically and found that at room temperature there is an equilibrium between several conformations with distinct aromaticities.[36] Doubly twisted Möbius-type porphyrinoids with figure-eight topologies can be stabilized by metalation forming bimetal complexes involving the two molecular loops.[36−42]

Latos-Grazyńsky et al. reported the synthesis of Möbius-stabilized porphyrinoids containing two pairs of pyrrolic units connected through benzene rings.[34,35,43] Two conformers were characterized in solution, one with stacked arene units forming a molecule with Hückel topology. The corresponding Möbius structure has the two phenylene rings perpendicularly oriented in a edge-to-face fashion. Shimizu et al. recently prepared twisted meso-trifluoromethyl-substituted hexaphyrins.[44] The aromaticity and topology of the doubly twisted [26]hexaphyrin and [28]hexaphyrin were studied computationally by Rzepa et al.[11,45,46] The studies of the molecular topology showed that the hexaphyrins are formally double-twisted molecules with L_k equal to 2. Measurements of the ^{1}H NMR chemical shifts for the NH hydrogens yielded a downfield shift for [28]hexaphyrin as also expected for hydrogens inside the paratropic current pathway of an antiaromatic molecule. However, the ^{1}H NMR signal for

the [26]hexaphyrin is unexpectedly shifted by 11.11 ppm in the same direction even though they, according to the generalized Hückel rule, should be aromatic.[44]

The article is organized as follows. In section 2, computational details such as employed methods, basis sets, and functionals are presented. In section 3, the calculated geometries, nuclear magnetic shieldings and shifts, and magnetically induced ring currents are given and analyzed. In section 4, the calculated ring currents are compared and discussed in detail. Finally the present work is summarized and concluded in section 5.

2. Computational Methods

The molecular structures were optimized at the density functional theory (DFT) level using Becke's three-parameter functional combined with the Lee−Yang−Parr exchange-correlation functional (B3LYP).[47,48] The molecular structures were fully relaxed using the Karlsruhe triple-ζ (def2-TZVP) basis set.[49] Nuclear magnetic shielding constants were calculated at the same level. Ring-current susceptibilities yielding ring-current strengths for a given value of the external magnetic field were calculated at the same level using a split-valence quality basis set augmented with polarization functions (def2-SVP).[49] The electronic structure calculations were performed with TURBOMOLE.[50−53] The magnetically induced current densities were obtained using the GIMIC method. GIMIC is an independent program that uses basis-set information as well as the perturbed and unperturbed density matrices from nuclear magnetic shielding calculations as input data.[1,54] Since gauge-including atomic orbitals (GIAO)[51,55−57] are used in the GIMIC approach, accurate current densities are obtained with double-ζ quality basis sets.[1]

The GIMIC method provides detailed information about molecular aromaticity.[6,7,9,58] The ring-current susceptibility, denoted in the following as ring-current strengths, can be used as a reliable measure of the molecular aromaticity. The current strengths are obtained by numerical integration of the current density passing through cut planes perpendicularly to selected bonds of the molecular system.[1] The ring-current strength for benzene calculated at the employed computational level is 11.9 nA/T and can be used as reference value. Calculations of the current strength for selected bonds yield the electron-delocalization pathways responsible for the current transport around the connected molecular rings. The current-density tensor is independent of the direction of the magnetic field, whereas contraction of the tensor with an external magnetic field makes the induced current density direction dependent. The sign and magnitude of the obtained ring currents indicate whether molecular rings are aromatic, antiaromatic, or nonaromatic thus having diatropic, paratropic, or vanishing net ring current, respectively.[10]

The strongest ring currents are obtained when the external magnetic field is largely perpendicular to the studied molecular ring. However, the twisted topology of the investigated molecules makes an unambiguous orientation of the direction of the magnetic field with respect to a selected bond difficult. Therefore, a careful investigation of the strength of the magnetically induced current with respect to the direction of the applied magnetic field is necessary for obtaining more thorough information about the degree of aromaticity of the molecule. The placement and size of the integration domain perpendicularly to the studied bond must also be chosen such that spurious current contributions from neighboring atoms are not considered. By assumption that the ring plane is oriented in the *xy* plane, the integration surface perpendicular to the ring can be chosen to lie in the *xz* plane. In the calculation of the current strengths, the applied magnetic field in the *xz* plane was rotated in steps of 15° from 0° to 180° starting from the negative *x* -axis making a clear assignment of the global aromatic character of the molecules according to the ring current criterion possible.

TABLE 1: Calculated Twisting (T_w), Writhing (W_r), and Linking (L_k) Numbers for the Molecular Structures of the Hexaphyrins Optimized at the B3LYP/def2-TZVP Level

molecule	T_w	W_r	L_k
(**1**)	1.31	0.69	2.0
(**2**)	0.98	1.02	2.0
(**3**)	1.02	0.98	2.0
(**4**)	1.06	0.94	2.0
(**5**)	1.20	0.80	2.0

3. Results and Discussion

3.1. Molecular Structures. Expanded porphyrins are macrocyclic molecules consisting of more than four pyrrole rings connected by conjugated bonds. They have unique chemical properties, as they are very flexible molecules with continuous π-conjugation around the porphyrin ring. Thus, they have the ability to form singly and multiply twisted Möbius aromatic and antiaromatic molecules.[28−32,36,44] The Möbius-twisted molecules can also be stabilized by metalation.[36−40] DFT optimization of the molecular structure of the hexaphyrins with six pyrrole units yielded doubly Möbius twisted molecules (L_k = 2) with about equal amount of twist (T_w) and writhe (W_r).[11,45,46] Thus, half of the twisting strain is compensated by forming a lemniscular shape of the molecular ring. See Table 1. Rzepa and Allan assumed the inner pathway in the calculation of the linking numbers for the hexaphyrins (**2**), (**3**), and (**4**), whereas the outer route was used in the present calculations of the topology numbers using the same software.[11] The obtained linking, twisting, and writhing numbers are largely equal showing that the topology is independent of the route adopted in the calculation, as one also would expect. The topology of the molecules suggests that [26]hexaphyrins (**2**) and (**3**) and [30]hexaphyrin (**5**) are aromatic because the expected aromatic pathway involves 26 and 30 π-electrons, respectively. Analogously, [24]hexaphyrin (**1**) and [28]hexaphyrin (**4**) should be antiaromatic according to Hückel's rule. A popular structural criterion for aromaticity is the bond-length alternation HOMA (harmonic oscillator model of aromaticity) index given by[59]

$$\mathrm{HOMA} = 1 - \frac{\alpha_{CC}}{n}\sum_i (R_{CC,opt} - R_{CC,i})^2 + \frac{\alpha_{CN}}{n}\sum_i (R_{CN,opt} - R_{CN,i})^2 \quad (1)$$

The α_{CC}, α_{CN}, $R_{CC,opt}$, and $R_{CN,opt}$ constants are taken from a previous study,[59] and *n* is the number of bonds forming the ring. For aromatic rings with little bond-length alternation (BLA), the HOMA index is about 1. Very small and negative HOMA values mean that the ring consists of localized single and double bonds suggesting that they are non- or antiaromatic.[59,60] The molecular structures of the hexaphyrins are shown in parts a−e of Figure 2. The Cartesian coordinates are given in the electronic Supporting Information.

The HOMA indices of the pyrrole rings and of different paths around the macroring differ for the studied hexaphyrins. The indices are rather unsystematic making the assessment of the

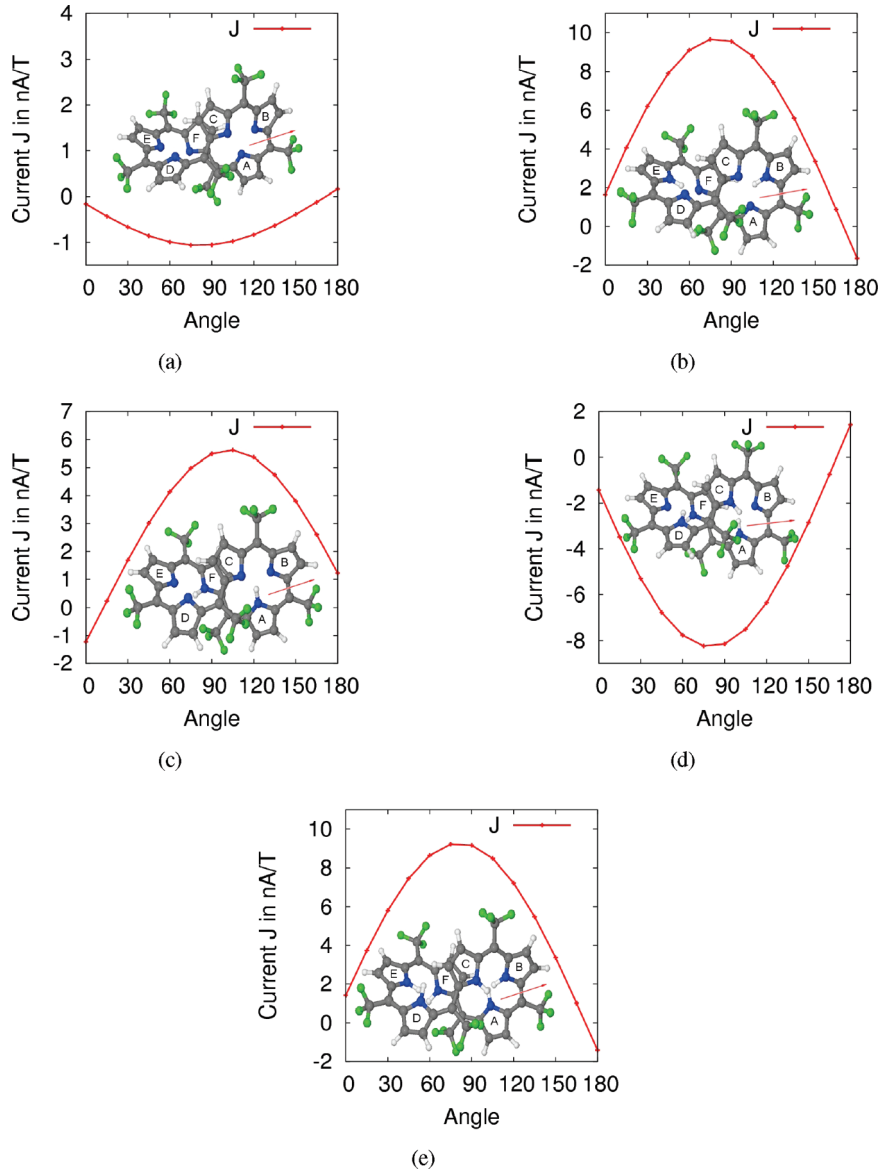

Figure 2. The employed nomenclature A−F of the pyrrole subrings of the hexaphyrins (**1**)−(**5**). The red curve shows the strength of the magnetically induced current of the hexaphyrins as a function of the direction of the external magnetic field. The angle is given in degrees. The bond where the integration is performed is indicated with the arrow. (a) The minimum of the current strength function is −1.1 nA/T. (b) The maximum of the current strength function is 9.6 nA/T. (c) The maximum of the current strength function is 5.6 nA/T. (d) The minimum of the current strength function is −8.2 nA/T. (e) The maximum of the current strength function is 9.2 nA/T.

TABLE 2: Value of the HOMA Index for the Pyrroles and for Various Paths in the Hexaphyrins

pyrrole or path	(**1**)	(**2**)	(**3**)	(**4**)	(**5**)
A	−0.04	0.31	0.80[a]	0.38[a]	0.65[a]
B	−0.07	0.74[a]	0.41	0.40	0.85[a]
C	−0.04	0.27	0.15	0.92[a]	0.72[a]
D	−0.04	0.25	0.11	0.38[a]	0.86[a]
E	−0.07	0.57[a]	0.15	0.41	0.64[a]
F	−0.04	0.22	0.56[a]	0.92[a]	0.88[a]
inner path	0.46	0.91	0.84	0.73	0.80
outer path	−0.30	0.35	0.29	0.45	0.79
classical path	0.46	0.78	0.75	0.57	0.79

[a] Hydrogenated pyrrole rings.

degree of aromaticity according to the structural criterion difficult. The HOMA indices listed in Table 2 indicate that the hydrogenated pyrrole rings have a larger electron delocalization and a smaller BLA than pyrrole rings with no hydrogen attached to the nitrogen. This holds especially for the aromatic hexaphyrins (**2**) and (**3**). The HOMA value of two of the four hydrogenated pyrrole rings in the antiaromatic hexaphyrin (**4**) is 0.92, while the rest of the pyrrole rings has similar HOMA values although two of them have the nitrogen atom hydrogenated and two have not. Hexaphyrin (**1**) has all pyrrole rings non-hydrogenated. The double bonds in the pyrrole rings of hexaphyrin (**1**) are essentially localized as the HOMA index is close to zero. Hexaphyrin (**5**) with all pyrrole rings hydrogenated has two kinds of pyrrole rings. According to the HOMA index, three of them have a larger electron delocalization. They have a small BLA corresponding to HOMA values of 0.85−0.88, whereas the HOMA values of other three pyrrole rings are 0.64−0.72. For the pyrrole rings of the hexaphyrins (**2**), (**3**), and (**4**), the HOMA values are scattered between 0.11 and 0.92. In general, the smallest HOMA values were obtained for the non-hydrogenated pyrrole rings. However, two of the four hydrogenated pyrrole rings of hexaphyrin (**4**) have smaller HOMA indices than for the non-hydrogenated ones. Thus,

determination of the degree of aromaticity from the HOMA indices of the pyrrole rings is nontrivial.

The aromatic character of the hexaphyrins is not determined solely by the BLA and HOMA indices of the individual pyrrole rings; the aromaticity of the hexaphyrins is a global property. The HOMA values calculated for different pathways around the hexaphyrin ring are also given in Table 2. The classical current path is taken as the one passing the pyrrole nitrogen when it is unhydrogenated. For hexaphyrin (**1**), the inner route coincides with the classical route, whereas for hexaphyrin (**5**) the classical conjugation pathway follows along the C═C route at all pyrrole rings. The HOMA value along the classical conjugation pathway is 0.46 and 0.57 for the formally antiaromatic hexaphyrins (**1**) and (**4**), and it is around 0.8 for the formally aromatic conjugation pathway of hexaphyrins (**2**), (**3**), and (**5**). Still larger HOMA values were obtained for the inner paths of hexaphyrins (**2**) and (**3**).

Herges showed that the magnetic aromaticity criterion and the HOMA index behave qualitatively different for aromatic and antiaromatic molecules.[19] He found unexpectedly that [16]annulene isomers having large positive nucleus independent chemical shifts (NICS) i.e., antiaromatic molecules according to the magnetic criterion, exhibit a smaller BLA than molecules with vanishingly small NICS values. However, the discrepancy between HOMA and magnetic aromaticity indicators can be rather easily understood. An aromatic or an antiaromatic molecular ring needs a continuous electron delocalization in order to sustain a ring current. It does not matter whether the ring current is diatropic or paratropic. The studied molecules sustaining paratropic ring currents also exhibit a reduced BLA as demonstrated by the small differences in the HOMA indices of the hexaphyrins (**2**), (**3**), and (**4**). Thus, the HOMA index might not be a very reliable aromaticity indicator, especially when one cannot easily judge whether the molecule sustains a diatropic or paratropic ring current.

Because the expanded porphyrins are structurally very flexible, the three-dimensional structures vary along the series. Especially in hexaphyrin (**4**), the two kinds of hydrogenated pyrrole rings, as identified by the HOMA indices, have different local surroundings. Hydrogen bonding to fluorine atoms seems to affect the ^{1}H NMR shieldings of the hydrogen atoms bonded to the nitrogen. The influence of steric effects on the BLA and HOMA values is more difficult to assess.

[26]Hexaphyrin and [28]hexaphyrin have 15 isomers with different positions of the inner hydrogens. Two of the [26]hexaphyrin isomers, molecules (**2**) and (**3**), were studied to get an insight into the effect of the different hydrogen positions on the ring currents. Low barriers for hydrogen transfer between the pyrrole sites have been found experimentally and computationally in porphyrins[61,62] and by means of ^{1}H NMR experiments for di-*p*-benzihexaphyrin,[34] implying a dynamical equilibrium of all 15 isomers at room temperature at least on the NMR time scale. Hexaphyrin (**2**) is 43 kJ/mol lower in energy than (**3**). This energy difference is of the same magnitude as previously seen for different conformers, with respect to the hydrogen positions, of bonellin-dimethylester.[62]

The relative energies of the investigated isomers provide a qualitative measure of the aromatic stabilization energies. The magnetically induced current strengths discussed below indicate that hexaphyrin (**1**) is nonaromatic while (**2**), (**3**), and (**5**) are aromatic and hexaphyrin (**4**) is antiaromatic. By adoption of this characterization, the sum of the total energies of (**1**) and (**4**) should be higher than the sum of the energies of (**2**) and (**3**). In this way an aromatic stabilization of [26]hexaphyrin with respect to the non- and antiaromatic [24] and [28]hexaphyrins of 135 ± 42.4 kJ/mol is obtained. The energies of hexapyrins (**2**) and (**4**) add up to 339 kJ/mol less than the sum of the energies for (**1**) and (**5**). The opposite is expected since hexaphyrin (**4**) should be destabilized due to its antiaromatic character. This discrepancy is to be seen in the light of the T_w and W_r components of the linking number L_k. For (**1**) and (**5**), the twisting numbers T_w are 1.31 and 1.20. The energy loss due to the twist is compensated by a W_r of 0.69 and 0.80, respectively. For hexaphyrins (**2**)−(**4**), the T_w and W_r components are approximately 1 implying that the π-overlap is overall larger as compared to (**1**) and (**5**). The ^{1}H NMR chemical shieldings discussed below indicate that intramolecular hydrogen bonding in (**4**) might stabilize it.

TABLE 3: ^{1}H NMR Shieldings (σ_H in ppm) of the NH Hydrogens of the Pyrrole Rings A−F as Depicted in Figure 2[a]

molecule	σ_{H_A}	σ_{H_B}	σ_{H_C}	σ_{H_D}	σ_{H_E}	σ_{H_F}
(**2**)		25.7			25.6	
(**3**)	20.6					21.1
(**4**)	12.2		17.1	12.2		17.1
(**5**)	28.7	28.6	27.4	28.6	29.2	26.5

[a] The shieldings were calculated at the B3LYP/def2-TZVP level. The free-base porphyrin value is 39.9 ppm.[66]

TABLE 4: ^{1}H NMR Shifts (δ_H in ppm, with Respect to TMS[a]) of the NH Hydrogens of the Pyrrole Rings A−F as Depicted in Figure 2[b]

Molecule	δ_{H_A}	δ_{H_B}	δ_{H_C}	δ_{H_D}	δ_{H_E}	δ_{H_F}	δ_{Exp}	δ_{Exp}
(**2**)		6.2			6.3			
(**3**)	11.3					10.8	10.3[c]	11.1[d]
(**4**)	19.7		14.1	19.7		14.1	4.11, 9.55[e]	12.35, 14.95[d]
(**5**)	3.2	3.3	4.5	3.3	2.7	5.4		

[a] The ^{1}H NMR chemical shielding for TMS is 31.91 ppm at the B3LYP/def2-TZVP level. [b] The shieldings were calculated at the B3LYP/def2-TZVP level. The calculated value for free-base porphyrin is −8.0 ppm.[66] [c] Reference 34 for the Möbius form of di-*p*-benzihexaphyrin. For the corresponding Hückel form, a ^{1}H NMR chemical shift of 16.51 ppm was reported. [d] Reference 44. [e] Reference 36.

3.2. Nuclear Magnetic Shieldings and Chemical Shifts. The ^{1}H NMR chemical shifts of the NH hydrogens of free-base porphyrin are shifted upfield because the hydrogens lie inside the ring current loop. For the aromatic hexaphyrins, one would also expect an upfield shift of the ^{1}H NMR signal of the NH hydrogens. However, the hexaphyrins have strongly twisted structures implying that the ring current contribution to the magnetic shielding constants is less predictable. Calculations of the ^{1}H NMR shieldings yielded significantly smaller values for the ^{1}H NMR shieldings than for free-base porphyrin. See Table 3. The calculated ^{1}H NMR shieldings are all downfield shifted as compared to tetramethylsilane (TMS). The ^{1}H NMR shielding of TMS is 31.9 ppm at the same computational level.[63] The ^{1}H NMR chemical shifts with respect to TMS are compared to experimental results[34,36,44] in Table 4. The variations in the experimental results reflect the difficulty to unambiguously relate a possible conformer to the measured NMR chemical shifts since the expanded porphyrins are very flexible. Furthermore, solvent effects have not been taken into account in our calculations. The calculated ^{1}H NMR chemical shieldings agree qualitatively with the experimental results. The calculations yielded the smallest ^{1}H NMR shieldings for the NH hydrogens of [28]hexaphyrin, as one would expect based on the paratropic ring current. Even though [26]hexaphyrin and [30]hexaphyrin sustain diat-

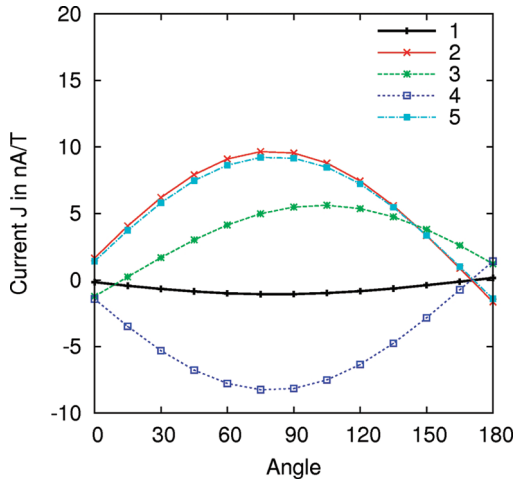

Figure 3. Comparison of the current strengths of the hexaphyrins (**1**)−(**5**) calculated as a function of the direction of the external magnetic field.

ropic ring currents, the ^{1}H NMR signals are downfield shifted as compared to TMS. For free-base chlorins and porphyrins, the ^{1}H NMR shieldings are in the range of 25−40 ppm, indicating the variation in the current strengths in them.[64]

The ring-current strengths and the ^{1}H NMR shieldings of the inner hydrogens correlate. The stronger the ring current is, the larger are the ^{1}H NMR shieldings of the NH hydrogens. Previously a strong correlation between the ^{1}H NMR shieldings of the inner hydrogens and current strengths has been established in hydrocarbon nanorings.[5] The strongly nonplanar structures of the hexaphyrins affect the ring-current contribution to the shieldings. The ^{1}H NMR shielding constant of the antiaromatic [28]hexaphyrin (**4**) is 5−10 ppm smaller than for hexaphyrin (**3**), which has the weakest diatropic ring current of the aromatic ones.

The two different ^{1}H NMR chemical shieldings in hexaphyrin (**4**) can not be explained by the induced currents. The large chemical shifts most likely arise from hydrogen bonding between the inner pyrrole hydrogen and a nearby fluorine atom. The inner hydrogens of the pyrrole rings with N−H···F distances in the hydrogen bonding regime of 193 pm have ^{1}H NMR shieldings of 12 ppm, whereas for the pyrrole N−H hydrogens with N−H···F distances of 225 pm the ^{1}H NMR shielding is 17 ppm.

3.3. Magnetically Induced Current Densities. The current strengths of selected covalent bonds of the six hexaphyrins were investigated. The aim of the current density calculations is to obtain an unambiguous identification of the ring-current pathways in the hexaphyrins with many feasible current routes. The ring current strengths were calculated as a function of the direction of the external magnetic field because nonplanar molecules have no obvious direction of the field. In Figure 2, the current strengths of the hexaphyrins (**1**)−(**5**) are given as a function of the angle of the external magnetic field, as described in section 2. The integration plane cuts the C−C bond between a pyrrole ring and a *meso*-trifluoromethane group, as illustrated in Figure 3. The parabolic shaped current-strength functions allow a clear assignment of the aromatic character of the investigated molecules.

For the current-density studies of the pyrrole rings, the direction of the external magnetic field was fixed at the angle that yielded the maximum or minimum current strength for the hexaphyrins with net diatropic or paratropic ring-current strengths, respectively. A comparison of the current strengths of the hexaphyrins calculated as a function of the angle of the external magnetic field is shown in Figure 3. The six pyrrole rings are named A−F as shown in parts a−e of Figure 2. The obtained current strengths passing the C−N−C or C=C moieties are given in Tables 5−9. The detailed ring-current calculations of the pyrrole rings reveal whether the current passes the C−N−C moiety or the pyrrole C=C bond, rendering

TABLE 5: Strengths of the Magnetically Induced Currents (in nA/T) Floating along the Outer (C=C) and Inner (C−N−C) Routes at the Pyrrole Rings of Hexaphyrin (1)[a]

pyrrole ring/path→	C−N−C	C=C
A	1.4	−1.7
B	2.0	−2.2
C	1.0	−1.0
D	−1.0	0.2
E	−0.2	−0.5
F	0.0	−1.1

[a] The A−F labeling of the pyrrole rings is given in Figure 2a. The minimum of the current strength function with respect to the angle of the applied magnetic field is −1.1 nA/T.

TABLE 6: Strengths of the Magnetically Induced Currents (in nA/T) Floating along the Outer (C=C) and Inner (C−N−C) Routes at the Pyrrole Rings of Hexaphyrin (2)[a]

pyrrole ring/path→	C−N−C	C=C
A	7.0	4.9
B	2.0[b]	9.8
C	6.9	4.3
D	9.8	0.3
E	6.8[b]	3.8
F	11.0	−0.6

[a] The A−F labeling of the pyrrole rings is given in Figure 2b. The maximum of the current strength function with respect to the angle of the applied magnetic field is 9.6 nA/T. [b] Hydrogenated pyrrole ring.

TABLE 7: Strengths of the Magnetically Induced Currents (in nA/T) Floating along the Outer (C=C) and Inner (C−N−C) Routes at the Pyrrole Rings of Hexaphyrin (3)[a]

pyrrole ring/path→	C−N−C	C=C
A	−0.7[b]	9.0
B	3.7	4.5
C	5.2	2.3
D	7.6	−1.1
E	6.2	0.6
F	6.3[b]	0.7

[a] The A−F labeling of the pyrrole rings is given in Figure 2c. The maximum of the current strength function with respect to the angle of the applied magnetic field is 5.6 nA/T. [b] Hydrogenated pyrrole ring.

TABLE 8: Strengths of the Magnetically Induced Currents (in nA/T) Floating along the Outer (C=C) and Inner (C−N−C) Routes at the Pyrrole Rings of Hexaphyrin (4)[a]

pyrrole ring/path→	C−N−C	C=C
A	−7.2[b]	−0.2
B	−8.6	1.8
C	−9.0[b]	1.6
D	−2.9[b]	−5.4
E	−5.1	−4.0
F	0.3[b]	−9.4

[a] The A−F labeling of the pyrrole rings is given in Figure 2e. The minimum of the current strength function with respect to the angle of the applied magnetic field is −8.2 nA/T. [b] Hydrogenated pyrrole ring.

TABLE 9: Strengths of the Magnetically Induced Currents (in nA/T) Floating along the Outer (C═C) and Inner (C—N—C) Routes at the Pyrrole Rings of Hexaphyrin (5)[a]

pyrrole ring/path→	C—N—C	C═C
A	0.7	10.3
B	−0.7	11.8
C	1.5	9.5
D	6.8	2.5
E	5.1	4.8
F	7.7	1.0

[a] The A—F labeling of the pyrrole rings is given in Figure 2e. The maximum of the current strength function with respect to the angle of the applied magnetic field is 9.2 nA/T.

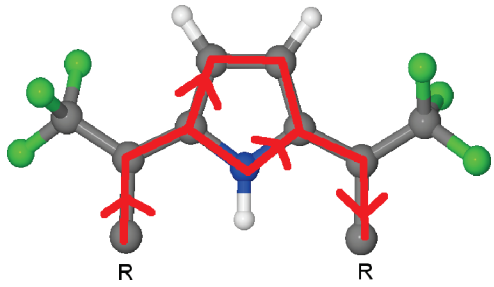

Figure 4. Schematic picture of the split ring current flow at a pyrrole subunit. The main hexaphyrin molecular ring is denoted by R.

determination of the current pathway feasible. Calculations of the current strengths at the pyrrole rings show whether the ring current is divided into two branches that join on the other side of the pyrrole ring as shown in Figure 4. Note that the pyrrole rings can also sustain their own ring currents.

3.3.1. [24]Hexaphyrin. [24]Hexaphyrin (**1**) is antiaromatic according to the Hückel rule. It has no inner hydrogens that could be used to assess its aromaticity experimentally. The molecular structure and the current strength calculated as a function of the external magnetic field are shown in Figure 2, respectively. The calculations show that practically no net current circles around the main molecular ring because the diatropic and paratropic contributions to the net ring current almost cancel, resulting in a very weak paratropic ring current. Hexaphyrin (**1**) must be considered nonaromatic according to the ring-current criterion. The pyrrole rings do not sustain any strong ring currents. The strongest ring current of the pyrrole rings is about 2.0 nA/T which is 6 times weaker than the one for benzene.

3.3.2. [26]Hexaphyrin. The molecular structures and the current-strength functions of the two Hückel aromatic isomers of [26]hexaphyrin (**2**) and (**3**) are shown in parts b and c of Figure 2. The two isomers have the inner hydrogens in different positions. For hexaphyrin (**2**), the pyrrole rings B and E are hydrogenated, whereas for hexaphyrin (**3**) the two inner hydrogens are attached to the pyrrole rings A and F. The main molecular ring of hexaphyrin (**2**) has a net ring-current strength of about 9.6 nA/T, which is almost the same as for benzene. For all pyrrole rings except B, the current is split into an inner route via C—N—C and an outer one via the pyrrole C═C bond. In general, the current has preference of the inner C—N—C pathway. For the hydrogenated pyrrole B, the current via the C═C bond is five times stronger than for the C—N—C route.

The calculations show that hexaphyrin (**3**) has largely similar current pathways and strengths as (**2**). Its net current strength of about 5.6 nA/T is 40% weaker than for (**2**). Pyrrole A, with an inner hydrogen, sustains a weak ring current of 0.7 nA/T. Pyrrole D sustains a weakly paratropic current of −1.1 nA/T. For (**3**), the main current flow passing pyrrole A occurs along the outer C═C route. The current is also split at rings C, D, E, and F, but for these pyrrole rings the inner C—N—C route is the dominant one. For pyrrole B without an inner hydrogen, the current is rather equally distributed between the inner and outer pathways. At pyrrole B, the flow via the C═C bond of 4.5 nA/T is slightly larger than the one of 3.7 nA/T along the inner path.

3.3.3. [28]Hexaphyrin. [28]Hexaphyrin (**4**) with four inner hydrogens is antiaromatic according to the Hückel rule. It has the pyrroles B and E non-hydrogenated. The molecular structure and ring-current-strength profile are given in Figure 2d. The calculations show that the ring current is paratropic with a net current strength of −8.2 nA/T. Thus, hexaphyrin (**4**) is antiaromatic according to the ring-current criterion. At the pyrrole rings D and E, the ring current is split, whereas the pyrrole rings B and C sustain weak ring currents of about 1.6 nA/T. For the pyrrole rings A, B, and C, the route over the inner C—N—C moiety is preferred, whereas the outer route via the C═C double bond dominates at the pyrrole F. At the pyrrole E, the current is almost equally split, though with a slight preference of the inner route. For pyrrole D, the current via the C═C bond is slightly stronger than the one through the C—N—C moiety.

3.3.4. [30]Hexaphyrin. [30]Hexaphyrin (**5**) having inner hydrogens at all six pyrroles is aromatic according to the Hückel rule. The molecular structure and the ring current profile are shown in Figure 2e. It sustains a net diatropic ring current, the strength of which is 9.2 nA/T. Thus, it is almost as aromatic as benzene according t the ring-current criterion. The main current takes the outer route along the C═C bond of the pyrrole rings A, B, and C, whereas the inner C—N—C route is preferred for pyrroles D, E, and F.

4. Discussion

The current pathways and the current strengths provide information about the electron delocalization and the aromaticity. In multiring molecules such as porphyrins and expanded porphyrins, the ring current can follow many possible routes. For example, previous current calculations on free-base porphyrin showed that the aromatic pathway involving 18 π-electrons is not the correct picture to understand its aromaticity.[1] The current calculations yielded a total ring current of 26 nA/T for the porphyrin ring. At the pyrrole rings, the current is forked. For the pyrroles with an inner H, the current strength along the C═C bond is 18 nA/T, whereas 8 nA/T flows via the inner route. For the pyrroles without an inner hydrogen, the corresponding current strengths are 12 and 14 nA/T, respectively. The current calculations showed that all 26 π-electrons of the free-base porphyrin take actively part in the current transport and contribute to its aromaticity. The ring-current pattern for hexaphyrins (**2**) and (**3**) reminds of that for free-base porphyrin in the sense that the ring current of the main molecular ring is divided into two branches at many of the pyrrole rings. The similarity in the ring currents of the two isomers of [26]hexaphyrin indicates that a detailed study of all possible isomers does most likely not provide any new insights.

Recent calculations on hydrocarbon nanorings showed the applicability of Hückel's rule to predict molecular aromaticity.[5] The hexaphyrins are another example where the Hückel rule provide a qualitative description of the aromatic character of the molecule. However, the Hückel rule cannot always be trusted as for some molecules we have found that the current densities do not obey the Hückel rule.[58,65] Current-density calculations

on polycyclic antiaromatic hydrocarbons yielded paratropic ring currents for molecules that should be aromatic according to the π-electron count showing the importance of current-strength calculations.[58] One explanation is that all π-electrons do not participate in the electron delocalization pathway, alternatively the π-electrons form independent aromaticity pathways.[5] Even though the *meso*-trifluoromethyl-substituted hexaphyrins are strongly twisted, the aromaticity can be estimated using the generalized Hückel π-electron rule. Antiaromatic hexaphyrins can though be nonaromatic rather than sustaining paratropic currents when they have too few electrons to form continuous electron delocalization pathways around the macroring. The formally antiaromatic hexaphyrin (**1**) with no inner hydrogens does not have enough electrons to sustain a strong paratropic ring current. Current calculations on hydrocarbon nanorings showed that the strength of the ring current of large molecular rings depends on the number of π-electrons participating in the current transport.[5] Especially, formally antiaromatic molecules prefer local currents instead of paratropic ring currents around the main molecular ring.

The current pathway at the pyrroles can either consist of an aromatic or antiaromatic ring current in the pyrrole ring combined with a global aromatic or antiaromatic current circling around the main molecular ring. The character of the ring current at the pyrrols can be obtained by determining the current path. The numerical integration of the current strengths passing the C—N—C and C═C moieties yields detailed information about the current pathway and its composition. A comparison of the curvature of the two paths with the curvature of the macroring in the vicinity of the investigated pyrrole shows whether the C═C or the C—N—C units belong to the inner or outer path, respectively. For the investigated hexaphyrins, the C—N—C moiety always belongs to the inner pathway, whereas for example inverted porphyrins have some of the C—N—C moieties oriented outward.

The gimic calculations lead largely to the same conclusions as recently reported by Rzepa and Allan,[45,46] who applied the NICS in combination with atoms in molecules (AIM) and electron localization function (ELF) critical point analyses. On the basis of bond analyses, they concluded that the C—N—C route better represents the conjugation pathway than the one via the outer C═C bonds of the pyrrole rings.[45] The present GIMIC calculations show that the aromatic pathway proposed by Rzepa and Allan does not always hold for the investigated hexaphyrins.[45,46] For the hexaphyrins (**2**), (**3**), and (**4**), Rzepa and Allen found that the current route through the C—N—C moiety dominates, which is also supported by the present calculations. The GIMIC calculations show that the current pathway of twisted molecules with many possible current routes cannot be reliably determined by employing NICS calculations.

For the aromatic hexaphyrins (**2**), (**3**), and (**5**), the ring current at the pyrroles can follow three routes. (i) The current can be split into diatropic currents along the outer C═C bond and via the inner C—N—C moiety. (ii) The current is diatropic along the C═C bond and paratropic via the C—N—C route, or iii) it is paratropic along the C═C path and diatropic via C—N—C. When the current both via the inner and the outer pathways is diatropic and of the same size, the ring current is divided into two branches as depicted schematically in Figure 4. This is probably the appropriate interpretation of the character of the current pathway when the currents of about equal size pass in the same direction via both routes. When the current strength of the outer C═C route is significantly larger than the one passing via the inner route, the pyrrole ring can be considered to sustain its own diatropic current. Analogously, when the current along the C═C moiety is much smaller than the inner one or a paratropic current passes the C═C bond, the pyrrole probably sustains its own paratropic ring current. However, the interpretation that the pyrrole rings are locally aromatic or antiaromatic is though somewhat arbitrary. For unclear situations, a more detailed study of the current pathway is needed to assess whether there is a change in the direction of the current flow at the pyrrole branching points.

For the antiaromatic hexaphyrins, the situation is very similar to the one for the aromatic ones. When the currents passing the C—N—C moiety and the C═C bond are of the same size and paratropic, the ring current is split into two branches at the pyrrole. The two other possibilities are identical for aromatic and antiaromatic hexaphyrins.

5. Summary and Conclusions

The magnetic behavior of doubly twisted *meso*-trifluoromethyl-substituted hexaphyrins have been investigated by performing explicit calculations of the aromatic electron delocalization pathways and ring current strengths. The current calculations at the DFT level show that the formal addition of electrons by increasing the number of inner hydrogens in steps of two yields alternating aromatic and antiaromatic molecules as long as the hexaphyrin ring has enough electrons for sustaining a magnetically induced ring current around the macroring. The calculations show that the doubly Möbius-twisted ($L_k = 2$) hexaphyrins with two (**2** and **3**) and six (**5**) inner hydrogens are aromatic, whereas the one with four inner hydrogens (**4**) is a doubly twisted antiaromatic Möbius molecule. The formally antiaromatic hexaphyrin with no inner hydrogens (**1**) does not have enough electrons to sustain a strong paratropic ring current and must therefore be considered to be nonaromatic according to the ring current criterion.

A detailed analysis of the current pathways shows that the current is split at the pyrrole rings. The current can either take the inner route via the C—N—C moiety or the outer one along the C═C bond. For the aromatic hexaphyrins (**2**) and (**3**), the current via the inner C—N—C route dominates. However, this does not hold for the aromatic hexaphyrin (**5**) whose main current follows the outer C═C route at the pyrroles A, B, and C. The inner C—N—C route dominates in the pyrroles D, E, and F. The molecular parts containing the pyrroles D, E, and F and the one with pyrroles A, B, and C are separated by twists of the hexaphyrin ring. For the antiaromatic hexaphyrin (**4**), the current pattern is almost the reverse. For the nonaromatic hexaphyrin (**1**) the weak paratropic current generally prefers the outer route via the C═C bond. The pyrrole rings do not sustain any strong ring current of their own.

Acknowledgment. This research has been supported by the Academy of Finland through its Centers of Excellence Programme 2006−2011. F.P. thanks the Global COE program of Tohoku University for financial support. We thank Prof. Rzepa for a copy of the linking-number program. We also thank CSC, the Finnish IT Center for Science, for computer time. The research in Karlsruhe has been supported by the Deutsche Forschungsgemeinschaft through the Center for Functional Nanostructures (CFN, Project No. C3.3). It has been further supported by a grant from the Ministry of Science, Research and the Arts of Baden-Württemberg (Az: 7713.14-300) and by the Fonds der Chemischen Industrie.

Supporting Information Available: The Supporting Information available contains the optimized Cartesian coordinates

of the investigated molecules and their total and relative energies, as well as the full ref 36. This material is available free of charge via the Internet at http://pubs.acs.org.

References and Notes

(1) Jusélius, J.; Sundholm, D.; Gauss, J. *J. Chem. Phys.* **2004**, *121*, 3952–3963.

(2) Zanasi, R.; Lazzeretti, P.; Malagoli, M.; Piccinini, F. *J. Chem. Phys.* **1995**, *102*, 7150–7157.

(3) Lazzeretti, P. *Prog. Nucl. Magn. Reson. Spectrosc.* **2000**, *36*, 1–88.

(4) Gomes, J. A. N. F.; Mallion, R. B. *Chem. Rev.* **2001**, *101*, 1349–1384.

(5) Taubert, S.; Jusélius, J.; Sundholm, D.; Klopper, W.; Fliegl, H. *J. Phys. Chem. A* **2008**, *112*, 13584–13592.

(6) Johansson, M. P.; Jusélius, J.; Sundholm, D. *Angew. Chem., Int. Ed.* **2005**, *44*, 1843–1846.

(7) Lin, Y. C.; Jusélius, J.; Sundholm, D.; Gauss, J. *J. Chem. Phys.* **2005**, *122*, 214308.

(8) Lin, Y. C.; Sundholm, D.; Jusélius, J.; Cui, L. F.; Li, X.; Zhai, H. J.; Wang, L. S. *J. Phys. Chem. A* **2006**, *110*, 4244–4250.

(9) Taubert, S.; Sundholm, D.; Pichierri, F. *J. Org. Chem.* **2009**, *74*, 6495–6502.

(10) Fliegl, H.; Sundholm, D.; Taubert, S.; Jusélius, J.; Klopper, W. *J. Phys. Chem. A* **2009**, *113*, 8668–8676.

(11) Rappaport, S. M.; Rzepa, H. S. *J. Am. Chem. Soc.* **2008**, *130*, 7613–7619.

(12) Călugăreanu, G. *Czech. Math. J.* **1961**, *11*, 588–625.

(13) Pohl, W. F. *Indiana Univ. Math. J.* **1968**, *17*, 975–985.

(14) White, J. H. *Am. J. Math.* **1969**, *91*, 693–728.

(15) Fuller, F. B. *Proc. Natl. Acad. Sci.* **1971**, *68*, 815–819.

(16) Wannere, C. S.; Rzepa, H. S.; Rinderspacher, B. C.; Paul, A.; Allan, C. S. M.; Schaefer III, H. F.; von Ragué Schleyer, P. *J. Phys. Chem. A* **2009**, *113*, 11619–11629.

(17) Hüeckel, E. *Grundzüge der Theorie Ungesättigter und Aromatischer Verbindungen*; Verlag Chemie: Berlin, 1938.

(18) von Eggers Doering, W.; Detert, F. L. *J. Am. Chem. Soc.* **1951**, *73*, 876–877.

(19) Herges, R. *Chem. Rev.* **2006**, *106*, 4820–4842.

(20) Ajami, D.; Hess, K.; Köhler, F.; Näther, C.; Oeckler, O.; Simon, A.; Yamamoto, C.; Okamoto, Y.; Herges, R. *Chem.−Eur. J.* **2006**, *12*, 5434–5445.

(21) Herges, R. *Nature* **2007**, *450*, 36–37.

(22) Ajami, D.; Oeckler, O.; Simon, A.; Herges, R. *Nature* **2003**, *426*, 819–821.

(23) Heilbronner, E. *Tetrahedron Lett.* **1964**, *5*, 1923–1928.

(24) Zimmerman, H. E. *J. Am. Chem. Soc.* **1966**, *88*, 1564–1565.

(25) Martín-Santamaría, S.; Lavan, B.; Rzepa, H. S. *J. Chem. Soc., Perkin Trans.* **2000**, *2*, 1415–1417.

(26) Castro, C.; Isborn, C. M.; Karney, W. L.; Mauksch, M.; von Ragué Schleyer, P. *Org. Lett.* **2002**, *4*, 3431–3434.

(27) Castro, C.; Chen, Z.; Wannere, C. S.; Jiao, H.; Karney, W. L.; Mauksch, M.; Puchta, R.; van Eikema Hommes, N. J. R.; von Ragué Schleyer, P. *J. Am. Chem. Soc.* **2005**, *127*, 2425–2432.

(28) Bauer, V. J.; Clive, D. L. J.; Dolphin, D.; Paine, J. B., III. *J. Am. Chem. Soc.* **1983**, *105*, 6429–6436.

(29) Setsune, J.; Maeda, S. *J. Am. Chem. Soc.* **2000**, *122*, 12405–12406.

(30) Shin, J. Y.; Furuta, H.; Igarashi, S.; Osuka, A. *J. Am. Chem. Soc.* **2001**, *123*, 7190–7191.

(31) Sprutta, N.; Latos-Grażyński, L. *Chem.−Eur. J.* **2001**, *7*, 5099–5112.

(32) Setsune, J.; Katakami, Y.; Iizuna, N. *J. Am. Chem. Soc.* **1999**, *121*, 8957–8958.

(33) Jux, N. *Angew. Chem., Int. Ed.* **2008**, *47*, 2543–2546.

(34) Stępień, M.; Latos-Grażyński, L.; Sprutta, N.; Chwalisz, P.; Szterenberg, L. *Angew. Chem., Int. Ed.* **2007**, *46*, 7869–7873.

(35) Stępień, M.; Szyszko, B.; Latos-Grażyński, L. *Org. Lett.* **2009**, *11*, 3930–3933.

(36) Sankar, J. et al. *J. Am. Chem. Soc.* **2008**, *130*, 13568–13579.

(37) Ahn, T. K.; Kwon, J. H.; Kim, D. Y.; Cho, D. W.; Jeong, D. H.; Kim, S. K.; Suzuki, M.; Shimizu, S.; Osuka, A.; Kim, D. *J. Am. Chem. Soc.* **2005**, *127*, 12856–12861.

(38) Saito, S.; Shin, J. Y.; Lim, J. M.; Kim, K. S.; Kim, D.; Osuka, A. *Angew. Chem., Int. Ed.* **2008**, *47*, 9657–9660.

(39) Tanaka, Y.; Saito, S.; Mori, S.; Aratani, N.; Shinokubo, H.; Shibata, N.; Higuchi, Y.; Yoon, Z. S.; Kim, K. S.; Noh, S. B.; Park, J. K.; Kim, D.; Osuka, A. *Angew. Chem., Int. Ed.* **2008**, *47*, 681–684.

(40) Yoon, Z. S.; Osuka, A.; Kim, D. *Nature Chem.* **2009**, *1*, 113–122.

(41) Saito, S.; Furukawa, K.; Osuka, A. *J. Am. Chem. Soc.* **2010**, *132*, 2128–2129.

(42) Lim, J. M.; Shin, J.-Y.; Tanaka, Y.; Saito, S.; Osuka, A.; Kim, D. *J. Am. Chem. Soc.* **2010**, *132*, 3105–3114.

(43) Latos-Grażyński, L. *Angew. Chem., Int. Ed.* **2004**, *43*, 5124–5128.

(44) Shimizu, S.; Aratani, N.; Osuka, A. *Chem.−Eur. J.* **2006**, *12*, 4909–4918.

(45) Rzepa, H. S. *Org. Lett.* **2008**, *10*, 949–952.

(46) Allan, C. S. M.; Rzepa, H. S. *J. Org. Chem.* **2008**, *73*, 6615–6622.

(47) Becke, A. D. *J. Chem. Phys.* **1993**, *98*, 5648–5652.

(48) Lee, C.; Yang, W.; Parr, R. G. *Phys. Rev. B* **1988**, *37*, 785–789.

(49) Weigend, F.; Ahlrichs, R. *Phys. Chem. Chem. Phys.* **2005**, *7*, 3297–3305.

(50) Ahlrichs, R.; Bär, M.; Häser, M.; Horn, H.; Kölmel, C. *Chem. Phys. Lett.* **1989**, *162*, 165–169.

(51) Wolinski, K.; Hinton, J. F.; Pulay, P. *J. Am. Chem. Soc.* **1990**, *112*, 8251–8260.

(52) Häser, M.; Ahlrichs, R.; Baron, H. P.; Weis, P.; Horn, H. *Theor. Chim. Acta* **1992**, *83*, 455–470.

(53) Kollwitz, M.; Häser, M.; Gauss, J. *J. Chem. Phys.* **1998**, *108*, 8295–8301.

(54) Ahlrichs, R.; Bär, M.; Häser, M.; Horn, H.; Kölmel, C. *Chem. Phys. Lett.* **1989**, *162*, 165–169.

(55) London, F. *J. Phys. Radium* **1937**, *8*, 397–409.

(56) Hameka, H. F. *Mol. Phys.* **1958**, *1*, 203–215.

(57) Ditchfield, R. *Mol. Phys.* **1974**, *27*, 789–807.

(58) Jusélius, J.; Sundholm, D. *Phys. Chem. Chem. Phys.* **2008**, *10*, 6630–6634.

(59) Krygowski, T. M. *Chem. Inf. Comput. Sci.* **1993**, *33*, 70–78.

(60) Cyrañski, M. K.; Krygowski, T. M.; Wisiorowski, M.; van Eikema Hommes, N. J. R.; von Ragué Schleyer, P. *Angew. Chem., Int. Ed.* **1998**, *37*, 177–180.

(61) Helaja, J.; Montfors, F. P.; Kilpeläinen, I.; Hynninen, P. H. *J. Org. Chem.* **1999**, *64*, 432–437.

(62) Sundholm, D.; Konschin, H.; Häser, M. *Chem.−Eur. J.* **1999**, *5*, 267–273.

(63) Taubert, S.; Konschin, H.; Sundholm, D. *Phys. Chem. Chem. Phys.* **2005**, *7*, 2561–2569.

(64) Jusélius, J.; Sundholm, D. *Phys. Chem. Chem. Phys.* **2000**, *2*, 2145–2151.

(65) Johansson, M. P. *J. Phys. Chem. C* **2009**, *113*, 524–530.

(66) Jusélius, J.; Sundholm, D. *Phys. Chem. Chem. Phys.* **1999**, *1*, 3429–3435.

JP1021517